Itraconazole Exerts Its Antitumor Effect in Esophageal Cancer By Suppressing the HER2/AKT Signaling Pathway

Wei Zhang[1,2,3,4], Ankur S. Bhagwath[1,5], Zeeshan Ramzan[1,5,6,7], Taylor A. Williams[1,2], Indhumathy Subramaniyan[8,9], Vindhya Edpuganti[8,9], Raja Reddy Kallem[8,9], Kerry B. Dunbar[1,5,6], Peiguo Ding[1,2], Ke Gong[10], Samuel A. Geurkink[11], Muhammad S. Beg[2,4], James Kim[2,3,4], Qiuyang Zhang[12], Amyn A. Habib[4,5,10], Sung-Hee Choi[2,5], Ritu Lapsiwala[2,5], Gayathri Bhagwath[2,5], Jonathan E. Dowell[2,4,5], Shelby D. Melton[1,5,13], Chunfa Jie[14], William C. Putnam[8,9,15], Thai H. Pham[1,5,16], and David H. Wang[1,2,3,4,5]

ABSTRACT

Itraconazole, an FDA-approved antifungal, has antitumor activity against a variety of cancers. We sought to determine the effects of itraconazole on esophageal cancer and elucidate its mechanism of action. Itraconazole inhibited cell proliferation and induced G_1-phase cell-cycle arrest in esophageal squamous cell carcinoma and adenocarcinoma cell lines. Using an unbiased kinase array, we found that itraconazole downregulated protein kinase AKT phosphorylation in OE33 esophageal adenocarcinoma cells. Itraconazole also decreased phosphorylation of downstream ribosomal protein S6, transcriptional expression of the upstream receptor tyrosine kinase HER2, and phosphorylation of upstream PI3K in esophageal cancer cells. Lapatinib, a tyrosine kinase inhibitor that targets HER2, and siRNA-mediated knockdown of HER2 similarly suppressed cancer cell growth *in vitro*. Itraconazole significantly inhibited growth of OE33-derived flank xenografts in mice with detectable levels of itraconazole and its primary metabolite, hydroxyitraconazole, in esophagi and tumors. HER2 total protein and phosphorylation of AKT and S6 proteins were decreased in xenografts from itraconazole-treated mice compared to xenografts from placebo-treated mice. In an early phase I clinical trial (NCT02749513) in patients with esophageal cancer, itraconazole decreased HER2 total protein expression and phosphorylation of AKT and S6 proteins in tumors. These data demonstrate that itraconazole has potent antitumor properties in esophageal cancer, partially through blockade of HER2/AKT signaling.

Introduction

Esophageal cancer is the sixth leading cause of cancer-related death and the eighth most common cancer worldwide (1). A rising incidence of esophageal cancer has led to an increasing burden on global health care systems. Because the majority of esophageal cancer patients present with advanced stage disease, the 5-year overall survival rate for patients of all stages is below 20% (2). There are two main histologic subtypes of esophageal cancer: esophageal squamous cell carcinoma (ESCC), which is predominantly found in the upper and middle thirds of the esophagus, and esophageal adenocarcinoma (EAC), which typically arises in the lower third of the esophagus. The incidence of EAC has increased dramatically in Western countries in the last few decades, coinciding with changes in the prevalence of its known risk factors. Whereas concomitant tobacco and alcohol consumption (risk factors for ESCC) has steadily decreased, gastroesophageal reflux disease, Barrett's esophagus, and obesity (risk factors for EAC) have rapidly increased (3, 4). Despite the different risk factors and pathobiology of ESCC and EAC, the clinical treatment of both is similar. Standard treatment for resectable esophageal cancer often involves a combination of surgery, chemotherapy, and radiotherapy (5). Two molecularly targeted therapies, trastuzumab (anti-HER2 antibody) and ramucirumab (anti-VEGFR2 antibody), and immune checkpoint blockade (ICB) are commonly used in combination with chemotherapy to treat advanced esophageal cancer (6–10).

The repurposing of existing medications for cancer treatment is becoming increasingly attractive because it can greatly reduce the cost and time required to develop novel therapeutics. Itraconazole is

[1]Esophageal Diseases Center, University of Texas Southwestern Medical Center, Dallas, Texas. [2]Division of Hematology-Oncology, Department of Internal Medicine, University of Texas Southwestern Medical Center, Dallas, Texas. [3]Hamon Center for Therapeutic Oncology Research, University of Texas Southwestern Medical Center, Dallas, Texas. [4]Harold C. Simmons Comprehensive Cancer Center, University of Texas Southwestern Medical Center, Dallas, Texas. [5]VA North Texas Health Care System, Dallas, Texas. [6]Division of Gastroenterology, Department of Internal Medicine, University of Texas Southwestern Medical Center, Dallas, Texas. [7]Department of Internal Medicine, TCU and University of North Texas Health Science Center School of Medicine and Texas Health Harris Methodist Hospital, Fort Worth, Texas. [8]Department of Pharmacy Practice, Texas Tech University Health Sciences Center, Dallas, Texas. [9]Clinical Pharmacology and Experimental Therapeutics Center, Jerry H. Hodge School of Pharmacy, Texas Tech University Health Sciences Center, Dallas, Texas. [10]Department of Neurology, University of Texas Southwestern Medical Center, Dallas, Texas. [11]Department of Internal Medicine, Methodist Dallas Medical Center, Dallas, Texas. [12]Department of Medicine, Center for Esophageal Diseases, Baylor University Medical Center, Dallas, Texas. [13]Department of Pathology, University of Texas Southwestern Medical Center, Dallas, Texas. [14]Department of Biochemistry and Nutrition, Des Moines University, Des Moines, Iowa. [15]Department of Pharmaceutical Science, Texas Tech University Health Sciences Center, Dallas, Texas. [16]Department of Surgery, University of Texas Southwestern Medical Center, Dallas, Texas.

Note: Supplementary data for this article are available at Molecular Cancer Therapeutics Online (http://mct.aacrjournals.org/).

Corresponding Author: David H. Wang, Division of Hematology-Oncology, Department of Internal Medicine, University of Texas Southwestern Medical Center, 5323 Harry Hines Blvd, MC 8852, Dallas, TX 75390–8852. Phone: 214-648-4180; Fax: 214-648-1955; E-mail: David1.Wang@UTSouthwestern.edu

Mol Cancer Ther 2021;20:1904–15

doi: 10.1158/1535-7163.MCT-20-0638

an antifungal drug with an established safety record. Over the last three decades, it has been widely used in the prevention and systemic treatment of a broad range of fungal infections. Early studies of the anticancer activity of itraconazole revealed its ability to inhibit the multidrug resistance associated protein P-glycoprotein at a low micromolar concentration (11, 12). Using a human endothelial cell proliferation assay, Liu and colleagues first identified itraconazole as an anti-angiogenic agent in 2007 through screening of a large panel of FDA-approved drugs (13). Kim and colleagues later showed that itraconazole is a potent antagonist of Hedgehog signaling (14). To date, a combination of *in vitro, in vivo*, and patient data in different tumor types has demonstrated that itraconazole possesses antitumor activity via diverse mechanisms including the aforementioned and initiation of cell cycle arrest, induction of autophagy and inhibition of PI3K/mTOR signaling (15, 16). On the basis of these observations and its well-established pharmacokinetic and toxicity profile, itraconazole has been tested in a number of human cancers. Clinical trials in basal cell carcinoma (17), prostate cancer (18), and non–small cell lung cancer (19, 20) have shown that itraconazole can increase progression-free survival in these patients. Retrospective studies further support the clinical benefits of itraconazole treatment in refractory malignancies including triple-negative breast cancer (21), ovarian cancer (22), and pancreatic cancer (23). Finally, itraconazole has multiple molecular targets so a potential added benefit is that it may have less acquired resistance than other drugs that target a single protein or pathway.

Few data are available on whether itraconazole has antitumor activity in esophageal cancer. A recent study showed that itraconazole inhibited growth of ESCC through activation of AMP-activated protein kinase (AMPK; ref. 24). Using a rat model of surgically-induced bile reflux that leads to Barrett's metaplasia, another study demonstrated that itraconazole significantly prevented progression of Barrett's esophagus to invasive EAC through targeting of the Hedgehog signaling pathway (25). Despite this, itraconazole's effects on human EAC have not been previously reported. In this study, we investigated whether itraconazole has antitumor effects on ESCC and EAC, and elucidated the underlying molecular mechanism. Using human esophageal cancer cell lines, xenografts in immunodeficient mice, and primary tumors from patients, we found itraconazole effectively inhibits esophageal cancer by targeting the HER2/AKT signaling pathway.

Materials and Methods

Cell lines and cell culture

The OE33 EAC cell line was purchased from Sigma in 2010; the FLO-1 EAC cell line was a generous gift of Dr. David Beer (University of Michigan, Ann Arbor, MI) in 2010; the KYSE70 and KYSE510 ESCC cell lines were generous gifts from Dr. John Harmon (Johns Hopkins University, Baltimore, MD) in 2006. OE33, FLO-1, KYSE70, and KYSE510 cells were cultured in RPMI1640 (Gibco) supplemented with 5% FBS (Hyclone), 100 U/mL penicillin/streptomycin, 2 mmol/L L-glutamine, and 10 mmol/L HEPES, and grown at 37°C in 5% CO_2 atmosphere. Two telomerase-immortalized esophageal squamous cell lines (NES-G2T and NES-B10T) and two telomerase-immortalized nondysplastic Barrett's epithelial cell lines (BAR-T and BAR-10T), generous gifts from Dr. Rhonda Souza (UT Southwestern, Dallas, TX) in 2009, were cultured as previously described (26). All cell lines were authenticated by DNA fingerprinting through the UT Southwestern McDermott Center DNA Genotyping Core and tested negative for *Mycoplasma*.

Cell proliferation assay

To evaluate the effect of itraconazole or lapatinib on cell proliferation, log-phase OE33, FLO-1, KYSE70, and KYSE510 cells were plated in 6-well plates at 1×10^5 cells/well and cultured in cell culture medium supplemented with 2.5 μmol/L itraconazole (Sigma), 2.5 μmol/L lapatinib (Cayman Chemical), or DMSO for up to 6 days, with replacement of medium and drug every 24 hours. Every 48 hours, cell proliferation was measured by using a hemocytometer, and each experiment was performed in triplicate. The cell viability assay was performed using AlamarBlue according to the manufacturer's protocol (Thermo Fisher Scientific). OE33 and KYSE510 cells were plated in Corning 96-well black plates with clear bottom at 1×10^3 cells/well and cultured in cell culture medium supplemented with 2.5 μmol/L itraconazole or DMSO for 72 hours. Fluorescence signal was measured at the designated timepoints under the fluorimeter (excitation at 544 nm and emission at 590 nm) using a POLARstar Omega Microplate Reader (BMG Labtech). Fluorescence signal was normalized to the cells treated with DMSO for 24 hours.

Western blot and antibodies

The cells were lysed in cell lysis buffer (50 mmol/L Tris-HCl, pH 8.0, 150 mmol/L NaCl, 0.5% sodium deoxycholate, 1% Triton X-100 plus protease and phosphatase inhibitors; Thermo Fisher Scientific; ref. 27). Overall, 20 μg of protein were run on 4%–12% Bis-Tris gels and transferred to polyvinylidene difluoride membranes. After blocking with 5% nonfat milk, the following antibodies were used to detect proteins: anti-phospho-AKT(S473) (#4060, Cell Signaling Technology), anti-phospho-AKT(T308) (#13038, Cell Signaling Technology), anti-AKT (#4691, Cell Signaling Technology), anti-phospho-S6 protein (#5364, Cell Signaling Technology), anti-S6 protein (#2217, Cell Signaling Technology), anti-phospho-PI3K p85 (#4228, Cell Signaling Technology), anti-PI3K p85 (#4257, Cell Signaling Technology), anti-phospho-AMPK-alpha (#2535, Cell Signaling Technology), anti-AMPK-alpha (#5831, Cell Signaling Technology), anti-PTEN (#9188, Cell Signaling Technology), anti-HER2 (#2165, Cell Signaling Technology), and anti-GAPDH (#ab2302, Millipore).

qRT-PCR

Total RNA was isolated with TRIzol (Thermo Fisher Scientific) and then reverse-transcribed using the Quantitect kit (Qiagen). Quantitative real-time PCR (qPCR) was performed using SYBR Green Master Mix (Thermo Fisher Scientific) on an Applied Biosystems StepOnePlus machine. Relative amounts of complementary DNA were calculated using the $\Delta\Delta C_t$ method and normalized to GAPDH. The primer sequences are as follows: CDK1 (F: 5′-AAACTACAGGTCAAGTGGTAGCC-3′; R: 5′-TCCTGCATAAGCACATCCTGA-3′), CDK2 (F: 5′-CCAGGAGTTACTTCTATGCCTGA-3′; R: 5′-TTCATCCAGGGGAGGTACAAC-3′), CDK4 (F: 5′-ATGGCTACCTCTCGATATGAGC-3′; R: 5′-CATTGGGGACTCTCACACTCT-3′), E2F1 (F: 5′-ACGTGACGTGTCAGGACCT-3′; R: 5′-GATCGGGCCTTGTTTGCTCTT-3′), HER2 (F: 5′-TGTGACTGCCTGTCCCTACAA-3′; R: 5′-CCAGACCATAGCACACTCGG-3′); GAPDH (F: 5′-TGGGCTACACTGAGCACCAG-3′; R: 5′-GGGTGTCGCTGTTGAAGTCA-3′).

siRNA

For gene knockdown experiments, OE33 or KYSE510 cells were transfected with either a nontargeting control (SC-37007, Santa Cruz Biotechnology) or ERBB2 targeting siRNA (SC-29405, Santa Cruz Biotechnology) using Lipofectamine LTX (Thermo Fisher Scientific). Cells were transfected at a 10 nmol/L siRNA concentration once and then transfected again 24 hours later. The cells were analyzed by

Western blot or cell proliferation assay 24 hours after the second transfection.

Tumor xenografts

To establish flank xenografts of OE33 cells, 5×10^6 cells suspended in 100 μL of PBS were mixed with 100 μL Matrigel (Corning), and subcutaneously injected into the flanks of female NOD-SCID mice. For itraconazole studies, when mice developed a palpable mass (≥200 mm^3), they were gavaged twice daily with oral itraconazole solution (Patriot Pharmaceuticals) 80 mg/kg for two weeks based on a prior study (14). Tumor size was measured twice a week with calipers, and volumes were determined using the formula (length × width × width)/2 (28).

IHC

IHC was performed on 4-μm–thick formalin-fixed, paraffin-embedded tissue sections. Antigen retrieval for deparaffinized tissue sections was performed in acidic citrate buffer for 20 minutes using a steamer. Following the blocking of endogenous peroxidase, paraffin-embedded sections were submitted to IHC staining using the Vectastain ABC system (Vector Laboratories) and visualized with DAB (Sigma; ref. 27). The anti-phospho-S6 protein (#5364, Cell Signaling Technology) was used at 1:1,000 dilution. IHC staining was reviewed by a board-certified pathologist (S.D. Melton).

Cell-cycle analysis

The cells were harvested by trypsin, washed with PBS twice, and then resuspended in 100% ice-cold ethanol for 4 hours. After that, the cells were resuspended in PBS with 50 μg/mL propidium iodide and 100 μg/mL RNase A for 1 hour. The DNA content was measured by flow cytometry, and percentages of cells in G_0–G_1, G_2–M, and S phases were calculated and analyzed by the software FlowJo (29).

Early phase I clinical trial

This window-of-opportunity clinical study was registered on clinicaltrials.gov (NCT02749513). In brief, patients with esophageal or gastroesophageal junction cancer deemed clinically resectable were approached for participation. Inclusion criteria were histologically proven ESCC, EAC, or gastroesophageal junction carcinoma. Exclusion criteria included presence of esophageal varices, symptomatic congestive heart failure, QTc > 450 ms, LFT's > 3X ULN, or allergy to itraconazole. Patients who provided written informed consent had initial pretreatment research biopsies collected at the time of diagnostic esophagogastroduodenoscopy (EGD) or staging endoscopic ultrasound (EUS; Supplementary Fig. S1). Up to eight biopsies of the tumor and three biopsies of uninvolved squamous epithelium were obtained with large forceps. Only patients with tumors with increased itraconazole targeted pathway activity compared with their normal squamous epithelium were prescribed itraconazole 300 mg to be taken orally twice daily for 14–17 days based on previous studies (18, 20). Up to eight posttreatment biopsies were collected at staging EUS (if pretreatment biopsies were obtained at diagnostic EGD) or a research EGD (if pretreatment biopsies were obtained at staging EUS) at the time of J-tube placement or laparoscopy for ischemic preconditioning (30). Pretreatment and posttreatment tumor biopsies were stained for phospho-S6 protein as described above. HER2 expression was determined by clinical assay using IHC and reflex FISH testing.

Itraconazole levels

Xenograft tumors and esophagi from NOD-SCID mice were collected and flash frozen on dry ice. The frozen tissue was homogenized by adding 4× volume of water using DPS-20 dual processing homogenizing system. A variable, measured volume of water was added to achieve smooth homogenate. Following homogenization, 20 μL of 2 mol/L ammonium acetate buffer was added to 50 μL of the tissue homogenate and the suspension was briefly vortexed. Extraction solvent (600 μL) containing 100 ng/mL posaconazole [Internal Standard (IS)] was added and vortexed for 30 minutes at 2,500 rpm. Following vortex mixing, the suspension was centrifuged 12,000 rpm for 5 minutes. Five-hundred microliters of the clear supernatant was removed, placed in a clean Eppendorf tube, and evaporated to dryness using a Labconco centrifugal vacuum concentrator. Samples were reconstituted using 200 μL of acetonitrile:water (70:30). Itraconazole and hydroxyitraconazole were quantified on a Sciex 5500 QTRAP LC/MS-MS system interfaced with a Shimadzu Nexera series UHPLC. Chromatographic separation was achieved by using a Kinetex C18 (1.7 μm, 2.1 × 50 mm) column with an injection volume of 5 μL using gradient elution. Quantitation was achieved by employing electrospray ionization in positive ion mode for the analytes in multiple-reaction monitoring mode. The analytic data obtained were processed using Sciex's Analyst software (version 1.7.1). Additional details are provided in the Supplementary Methods section.

Human phospho-kinase array

Human phospho-kinase array (#ARY003B, R&D Systems) was used according to the manufacturer's instructions and analyzed using the R&D Array HLImage++ software package. The pixel density of each spot was measured by the software and normalized to reference spots, then averaged for comparison. The identity and the respective coordinates of all the antibodies on the arrays are found at https://resources.rndsystems.com/pdfs/datasheets/ary003b.pdf.

Statistical analysis

Student *t* test was used for statistical analysis of the differences between the mean values of two groups. The tumor volume data were analyzed with a linear model of mixed effects for repeated measures, which accounts for the fixed effects (time and treatments) and their interaction as well as the random subject effects of the mice. By the Akaike information criterion (AIC) criteria, the unstructured covariance was selected over first-order autocorrelation and compound symmetry as the optimal covariance structure to account for the within-subject correlations. Bonferroni method was used to adjust the *P* values for the multiple comparisons with the R function glht.

Study approval

All animal experiments were approved by the Institutional Animal Care and Use Committee of the VA North Texas Health Care System prior to initiation. Human subjects research was conducted according to the principles embodied in the Declaration of Helsinki and was initiated only after approval by the Institutional Review Board of the VA North Texas Health Care System. Prior to enrollment in the human clinical trial, all study participants signed written informed consent.

Results

Itraconazole inhibits proliferation of esophageal cancer cells

To evaluate the effects of itraconazole on esophageal cancer, we utilized two different methods to measure cell growth. First, cell proliferation assays were performed on the representative EAC cell line OE33 and ESCC cell line KYSE510. The cells were treated with 2.5 μmol/L itraconazole or DMSO as vehicle control for 6 days. Cell

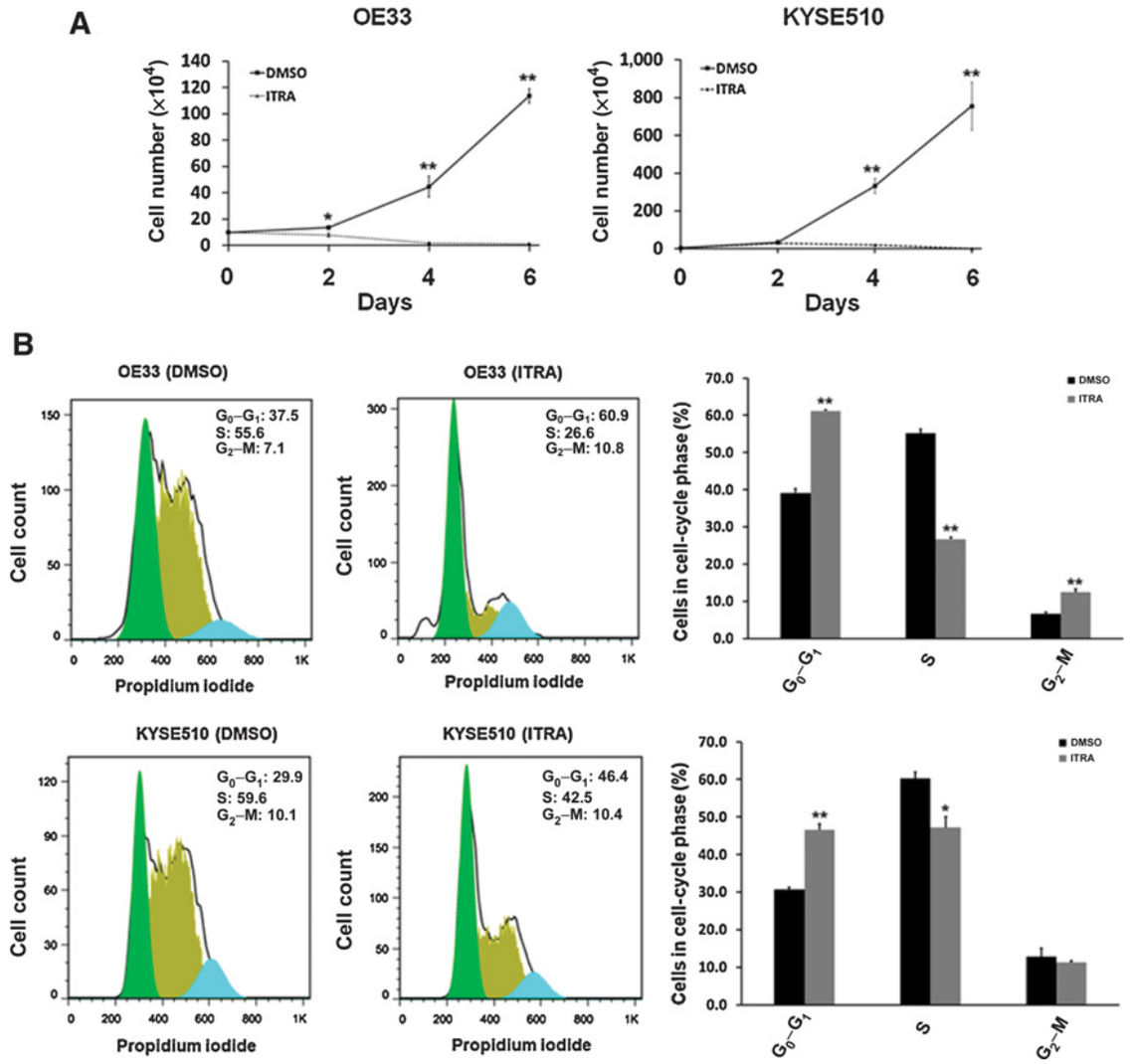

Figure 1.

Itraconazole inhibits proliferation of esophageal cancer cells. **A,** Cell proliferation assay for OE33 and KYSE510 cells. OE33 and KYSE510 cells were plated in 6-well plates and cultured in medium supplemented with 2.5 μmol/L itraconazole or DMSO for 6 days. Cell numbers were measured at the indicated timepoints. Values represent the mean ± SEM for triplicate wells. *, $P < 0.05$; **, $P < 0.01$ versus control group by Student *t* test. **B,** Representative cell-cycle analysis using flow cytometry after staining with propidium iodide. OE33 and KYSE510 were treated with 2.5 μmol/L of itraconazole or DMSO for 24 hours. Flow cytometric histograms of each phase of the cell cycle in OE33 or KYSE510 cells after itraconazole treatment as compared with control. Values represent the means ± SEM for three replicates. Black bars, DMSO; gray bars, itraconazole. *, $P < 0.05$; **, $P < 0.01$ versus control group by Student *t* test.

numbers at the indicated timepoints were counted. As shown in **Fig. 1A**, itraconazole started to exhibit a potent inhibitory effect by 48 hours after drug treatment, and this effect lasted until the end of the experiment in both OE33 and KYSE510 cells. The inhibitory effect of intraconazole on OE33 and KYSE510 cell proliferation was then confirmed by AlamarBlue assay (Supplementary Fig. S2). Second, we assessed the effects of itraconazole on the cell cycle in esophageal cancer cell lines because inhibition of cell proliferation often accompanies changes in cell-cycle progression. OE33 and KYSE510 cells were treated with 2.5 μmol/L itraconazole or DMSO for 24 hours, and cells were then collected for flow cytometric analysis based on propidium iodide staining of DNA content. The proportion of cells in G_0–G_1, S and G_2–M phases of the cell cycle was estimated using FlowJo software. After treatment with itraconazole for 24 hours, the cell-cycle distribution significantly changed with an increase in cell population in G_0–G_1 phase and a decrease in cell population in S-phase (**Fig. 1B**). In OE33 cells, the G_0–G_1 phase fraction increased from 37.5% (DMSO treated) to 60.9% (itraconazole treated). A similar trend was observed in KYSE510 cells with an increase in G_0–G_1 phase fraction from 29.9% (DMSO treated) to 46.4% (itraconazole treated). The itraconazole-induced cell growth inhibition and cell-cycle arrest at the G_1–S phase has been observed in other cancer types including gastric and breast cancer (31, 32). Together, our results demonstrate a potent inhibitory effect of itraconazole on esophageal cancer cell proliferation.

Itraconazole suppresses AKT activity in esophageal cancer

Oncogenic signaling mediators regulate cancer cell proliferation and cell-cycle progression. Thus, we postulated that itraconazole-

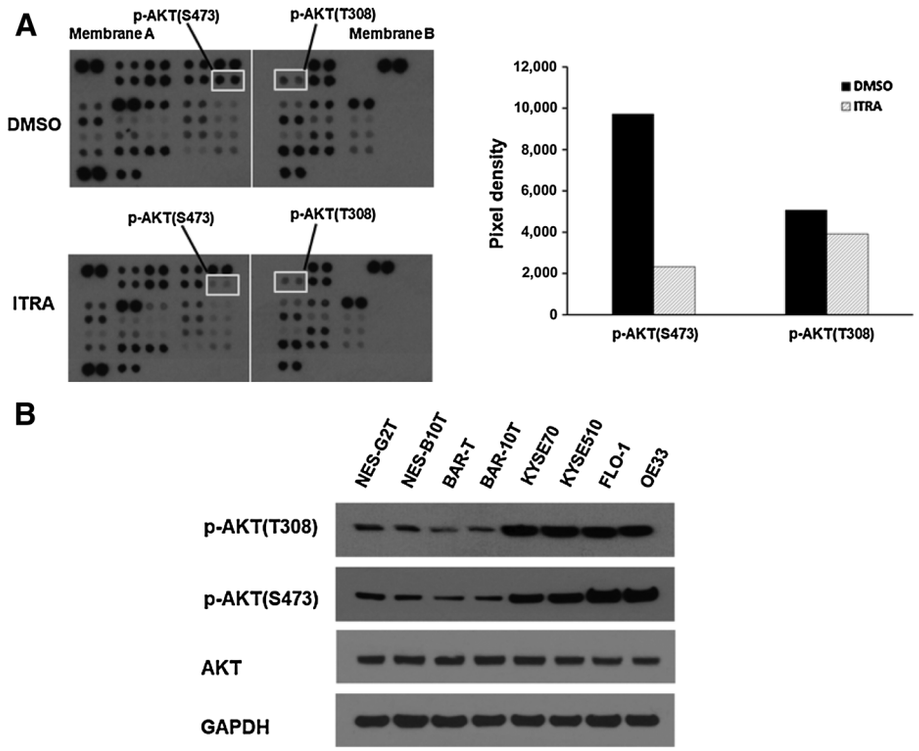

Figure 2.
Itraconazole suppresses AKT phosphorylation in esophageal cancer cells. **A,** Phospho-kinase analysis of OE33 cells treated with 2.5 μmol/L itraconazole or DMSO for 48 hours. The pixel density of marked phosphorylated AKT (left) relative to internal control is shown graphically (right). **B,** Upregulation of AKT activity in esophageal cancer. Western blot analysis of phosphorylated and total AKT expression in immortalized human esophageal squamous (NES-G2T, NES-B10T), Barrett's esophagus (BAR-T and BAR-10T), ESCC (KYSE70 and KYSE510), and EAC (FLO-1 and OE33) cell lines. GAPDH is used as a loading control.

mediated esophageal cancer cell growth might be due to suppression of key oncogenic signaling mediators. To test this hypothesis, we used an antibody-based phospho-kinase array to analyze the activation status of important signaling mediators in OE33 cells treated with 2.5 μmol/L itraconazole or DMSO for 48 hours. We chose 48 hours into treatment because itraconazole showed clear inhibitory activity on OE33 cell proliferation at this timepoint as shown in **Fig. 1**. Of the over 40 proteins evaluated, dramatic reduction of phosphorylation of AKT protein was observed (**Fig. 2A**). AKT is a serine/threonine kinase also known as protein kinase B (PKB), which plays a crucial role in major cellular functions including cell proliferation, cell-cycle progression, cell survival, transcription, and protein synthesis (33, 34). AKT can be phosphorylated at Thr308 and Ser473 in response to growth factor stimulation. Phosphorylation at both sites is required to achieve maximal activation of AKT and thus are considered markers of AKT activity (35). Notably, we found the phosphorylation status at both sites were reduced upon itraconazole treatment (**Fig. 2A**). Aberrant activation of AKT is a prevalent phenomenon in numerous cancer types. To examine the AKT status in esophageal cancer, we measured the level of phospho-AKT protein in two telomerase immortalized human esophageal squamous cell lines (NES-G2T, NES-B10T), two telomerase immortalized nondysplastic Barrett's esophagus cell lines (BAR-T and BAR-10T), two ESCC cell lines (KYSE70 and KYSE510), and two EAC cell lines (FLO-1 and OE33). The phosphorylation of AKT protein was increased in both ESCC and EAC cells compared with esophageal squamous or Barrett's esophagus cell lines (**Fig. 2B**).

To investigate whether itraconazole-mediated downregulation of AKT phosphorylation occurs in other esophageal cancer cell lines, we treated two EAC cell lines (OE33 and FLO-1) and two ESCC cell lines (KYSE70 and KYSE510) with 2.5 μmol/L itraconazole for 48 hours. Cell extracts from each cell line were subjected to SDS-PAGE and Western blot for AKT protein. Consistent with the antibody-based phospho-kinase array, itraconazole treatment reduced phosphorylation of AKT at both Thr308 and Ser473 sites in all four cell lines examined (**Fig. 3A**). After AKT is phosphorylated and activated, it executes diverse biological actions by phosphorylating a range of downstream proteins including the substrate mTOR. mTOR is a key component of the AKT signaling pathway, and it acts by directly phosphorylating and activating p70S6 kinase (p70S6K). Activated p70S6K phosphorylates the ribosomal protein S6, leading to initiation of protein synthesis (34). Ribosomal protein S6 is one of the best-characterized downstream effectors of AKT signaling, and it is required for cell-cycle progression at the G_1–S transition. To determine whether the itraconazole-mediated reduction of AKT phosphorylation affects downstream AKT signaling proteins, we examined the phosphorylation of ribosomal protein S6. We found itraconazole inhibited the phosphorylation of S6 protein in all four cell lines, indicating reduced AKT phosphorylation and activation had functional consequences in esophageal cancer cells, including the cell-cycle arrest observed in **Fig. 1B**.

To assess the functional relevance of AKT signaling in the context of itraconazole-mediated inhibition on esophageal cancer cell growth, we examined the transcriptional expression levels of AKT signaling target genes *CDK1, CDK2, CDK4*, and *E2F1* by reverse transcriptase–qPCR (RT–qPCR) analysis of OE33, FLO-1, KYSE70 and KYSE510 cells treated with itraconazole for 48 hours. We found itraconazole treatment led to significant reduction of *CDK1, CDK2, CDK4* and *E2F1* gene expression in OE33, FLO-1, KYSE70, and KYSE510 cells as shown in **Fig. 3B**. Collectively, our results point to a potent inhibitory effect of itraconazole on esophageal cancer via targeting AKT signaling.

Itraconazole downregulates HER2 expression in esophageal cancer

In response to growth factors, PI3K is the major activator of AKT. Because aberrant activation of PI3K/AKT signaling regulates cancer

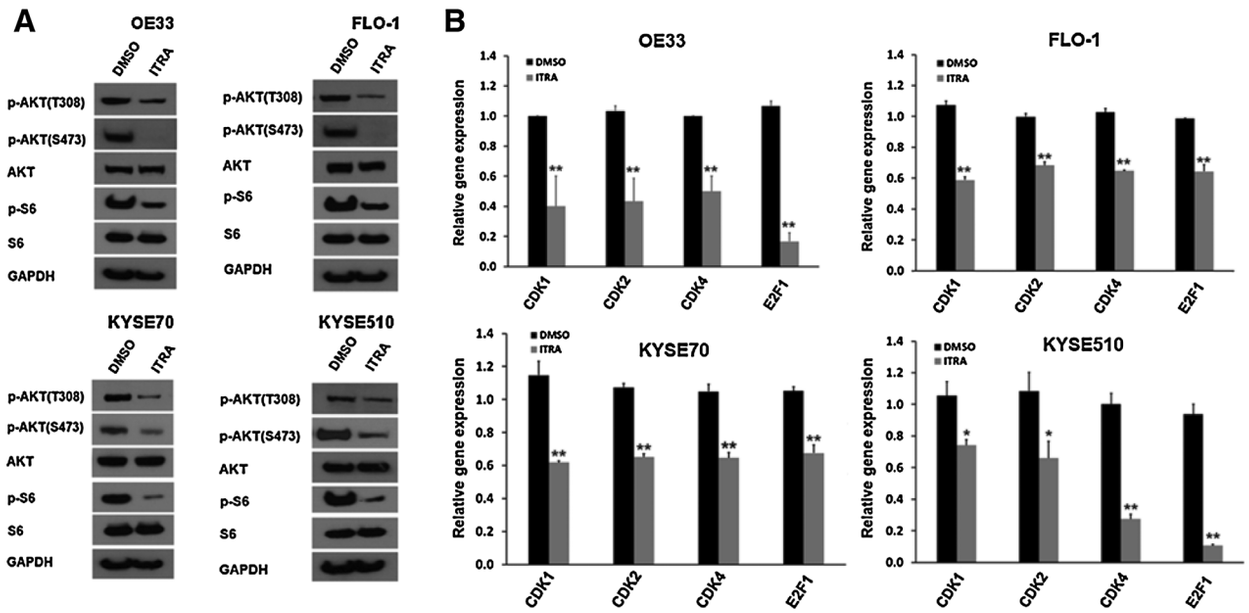

Figure 3.

Itraconazole inhibits AKT activity in both EAC and ESCC cell lines. **A,** Western blot analysis of p-AKT (Thr308 and Ser473), AKT, p-S6, and S6 expression in OE33, FLO-1, KYSE70, and KYSE510 cells treated with 2.5 μmol/L itraconazole or DMSO for 48 hours. GAPDH is used as a loading control. **B,** RT–qPCR analysis of *CDK1, CDK2, CDK4*, and *E2F1* genes in OE33, FLO-1, KYSE70, and KYSE510 cells treated with 2.5 μmol/L itraconazole or DMSO for 48 hours. Values represent the mean fold change ± SEM for three experiments relative to GAPDH. Black bars, DMSO; gray bars, itraconazole. *, $P < 0.05$; **, $P < 0.01$ vs. DMSO control by Student *t* test.

cell survival and proliferation, we next investigated whether the activity of PI3K is affected by itraconazole treatment. OE33, FLO-1, KYSE70 and KYSE510 cells were treated with itraconazole for 48 hours and assayed for PI3K activity based on its phosphorylation status. We found that itraconazole treatment impaired the activity of PI3K as indicated by the reduced phosphorylation of PI3K in four esophageal cancer cell lines (**Fig. 4A**).

It is well established that the canonical pathway leading to AKT activation is initiated by the stimulation of receptor tyrosine kinases (RTK) leading to plasma membrane recruitment and activation of PI3K family proteins. HER2 is one of the RTK associated with the development, progression, and metastases of several solid tumors including esophageal cancer. Next, we investigated whether HER2 status is responsible for the decreased level of PI3K phosphorylation. Indeed, our results indicated that itraconazole treatment led to down-regulation of HER2 protein in OE33, FLO-1, KYSE70, and KYSE510 cells (**Fig. 4A**). Moreover, we also compared *ERBB2* mRNA levels in OE33, FLO-1, KYSE70, and KYSE510 cells treated with itraconazole or DMSO for 48 hours. RT-qPCR revealed that *ERBB2* mRNA levels were significantly decreased following itraconazole treatment in all four esophageal cancer cell lines (**Fig. 4B**). Next, we found that the level of tumor suppressor PTEN, a major negative regulator of PI3K, was unchanged (**Fig. 4A**). A recent study suggested that activation of AMPK is involved in the inhibitory effects of itraconazole in ESCC (24). AMPK is a crucial energy sensor that regulates energy metabolism and mitochondrial homeostasis. AMPK can also be rapidly phosphorylated and activated in response to changes in the ATP-to-AMP ratio (36). Therefore, we also examined AMPK status in these four cell lines by Western blot. In contrast to the previous report, we did not see itraconazole activate AMPK as its phosphorylation did not increase (**Fig. 4A**). In fact, AMPK phosphorylation was even slightly reduced after itraconazole treatment for 48 hours particularly in KYSE70 and KYSE510 cells.

Finally, we decided to determine whether targeting HER2 has any effects on AKT activation status. Lapatinib is a HER2 tyrosine kinase inhibitor (TKI) that has clinical activity in HER2-amplified breast cancer. We found that 2.5–5.0 μmol/L lapatinib decreased AKT phosphorylation at S473 in OE33, KYSE510, FLO-1, and KYSE70 cells (**Fig. 4C**; Supplementary Fig. S3A). Next, we sought to determine whether inhibition of HER2 via lapatinib treatment could suppress esophageal cancer cell proliferation. OE33, KYSE510, FLO-1, and KYSE70 cells were treated with 2.5 μmol/L lapatinib for six days. Similar to itraconazole treatment, lapatinib reduced cell proliferation in OE33, KYSE510, FLO-1, and KYSE70 cells (**Fig. 4D**; Supplementary Fig. S3B). To confirm these findings, we then performed siRNA-mediated knockdown of HER2 in OE33 EAC and KYSE510 ESCC cells. After 72 hours, HER2 expression was decreased in cells transfected with HER2-specific siRNAs versus nontargeting siRNAs (**Fig. 4E**). We also found decreased downstream AKT phosphorylation. Cells treated for 72 hours with HER2 and nontargeting siRNAs were then analyzed using AlamarBlue assay, which demonstrated that HER2 knockdown decreased OE33 and KYSE510 cell proliferation (**Fig. 4F**). Taken together, itraconazole inhibits AKT activity via a HER2–PI3K–AKT axis in esophageal cancer cells.

Itraconazole inhibits esophageal cancer cell growth *in vivo*

To test the *in vivo* efficacy of itraconazole on esophageal cancer, NOD-SCID mice were subcutaneously implanted with OE33 cells on their flanks and randomly divided into 2 groups. Once the xenografts reached approximately 200 mm^3, the mice were treated with PBS as placebo or itraconazole (80 mg/kg) by oral gavage twice daily for 2 weeks. The tumor volume was measured at the indicated timepoints.

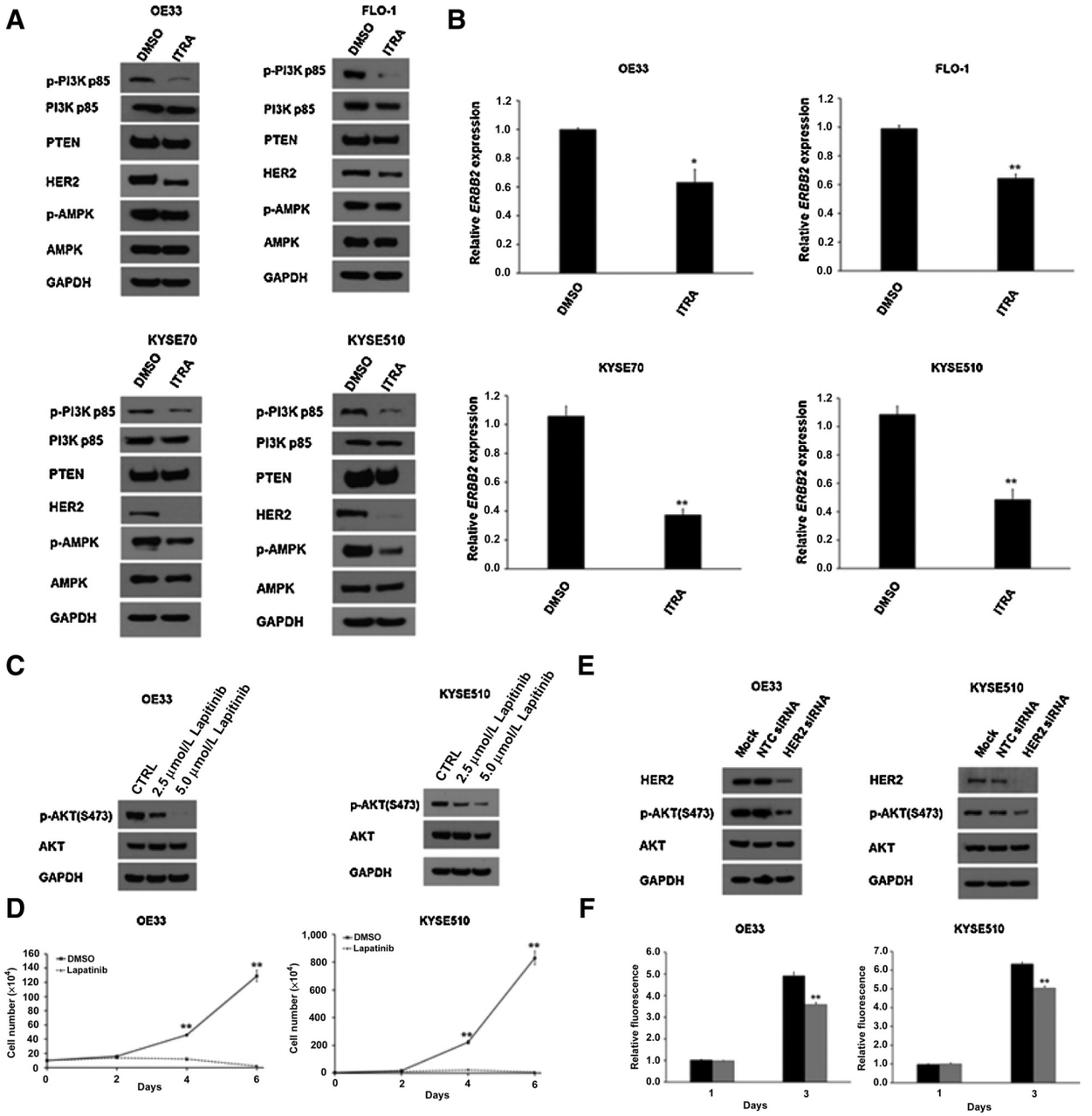

Figure 4.

Itraconazole inhibits HER2/PI3K signaling in esophageal cancer. **A,** Western blot analysis of p-PI3K, PI3K, PTEN, HER2, p-AMPK, and AMPK expression in itraconazole or DMSO-treated OE33, FLO-1, KYSE70 and KYSE510 cells. GAPDH is used as a loading control. **B,** RT–qPCR analysis of *ERBB2* mRNA levels in OE33, FLO-1, KYSE70 and KYSE510 cells treated with 2.5 μmol/L itraconazole or DMSO for 48 hours. Values represent the mean fold change ± SEM for three experiments relative to GAPDH. *, $P < 0.05$ and **, $P < 0.01$ versus control group by Student *t* test. **C,** Western blot analysis of p-AKT and AKT expression in OE33 and KYSE510 cells treated with DMSO, 2.5 μmol/L or 5 μmol/L lapitinib for 48 hours. GAPDH is used as a loading control. **D,** Cell proliferation assay for OE33 and KYSE510 cells treated with 2.5 μmol/L lapatinib. Cell numbers were counted at the indicated timepoints. The data are presented as the means ± SEM of three independent experiments. **E,** Western blot analysis of HER2, p-AKT, and AKT expression in OE33 and KYSE510 cells transfected with HER2-specific or NTC siRNAs for three days. GAPDH is used as a loading control. **F,** AlamarBlue-based cell proliferation assay for OE33 and KYSE510 cells treated with HER2-specific or NTC siRNAs for three days. Values represent the mean ± SEM for 8 wells. **, $P < 0.01$ versus control group by Student *t* test.

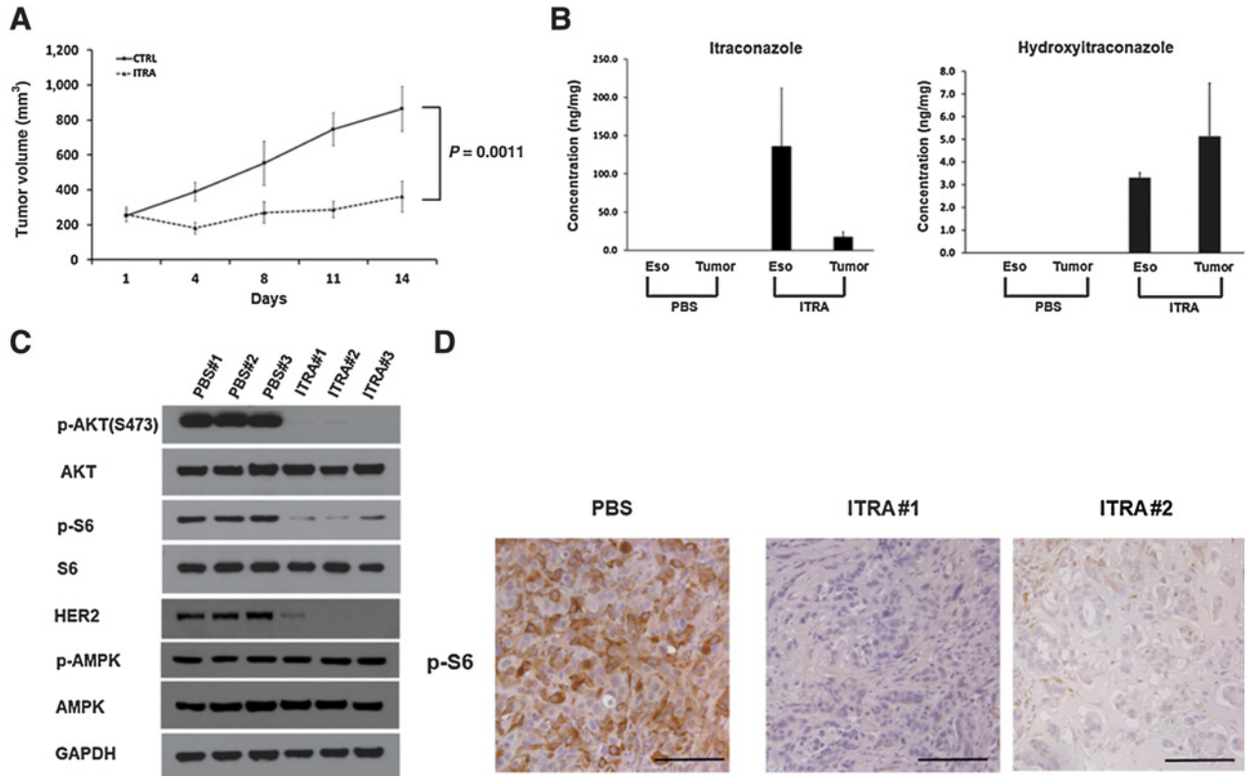

Figure 5.

Itraconazole inhibits OE33-derived tumor xenograft growth. **A,** NOD-SCID mice were injected subcutaneously with 5×10^6 OE33 cells. When tumors formed, mice were randomly divided into 2 groups (control and itraconazole, $n = 8$). The mice were treated with placebo or itraconazole (80 mg/kg) by oral gavage twice daily for two consecutive weeks. **B,** Concentrations of itraconazole and its primary metabolite hydroxyitraconazole in esophagi and tumor xenografts from mice treated with placebo or itraconazole. **C,** Western blot analysis of p-AKT, AKT, p-S6, S6, HER2, p-AMPK, and AMPK expression in OE33-derived xenografts treated with PBS or itraconazole for two weeks. GAPDH is used as a loading control. **D,** Representative IHC staining of p-S6 from xenograft sections treated with placebo or itraconazole. Scale bar, 100 μm.

As shown in **Fig. 5A**, oral administration of itraconazole significantly suppressed tumor growth *in vivo* compared with placebo. Itraconazole undergoes extensive metabolism by the cytochrome P450 system in the liver to generate its main active metabolite hydroxyitraconazole. To confirm the direct contribution of itraconazole to the tumor suppressive effect on OE33-derived xenografts, we measured the levels of itraconazole and hydroxyitraconazole in the xenografts from mice treated with itraconazole. Using an established method, we detected itraconazole and hydroxyitraconazole in the tumors treated with itraconazole, but not in the mice treated with placebo (**Fig. 5B**). Because our ultimate goal is to treat patients with esophageal cancer, we also measured the concentration of itraconazole and hydroxyitraconazole in the normal esophagus of mice using the same method. Similar to the tumor xenografts, both itraconazole and hydroxyitraconazole were detected in the esophagus of mice treated with itraconazole. In contrast, they were not detected in the esophagus and tumor xenografts from the mice treated with placebo (**Fig. 5B**). The underlying molecular mechanism of esophageal cancer inhibition *in vivo* was assessed by measuring the expression levels of HER2-AKT signaling pathway components in the tumor xenografts. In comparison to placebo-treated tumors, we noticed markedly reduced levels of HER2 total protein and AKT and downstream S6 protein phosphorylation (**Fig. 5C**). In addition, we did not see an increased level of AMPK activation as indicated by its phosphorylated protein levels. These results are consistent with our previous observations *in vitro*. Phosphorylated S6 protein as a marker of AKT activity was also evaluated in xenografts treated with placebo or itraconazole by IHC. Consistent with the Western blot results, phosphorylated S6 protein positive cells were markedly reduced in itraconazole-treated xenografts compared with placebo (**Fig. 5D**). Together, these data further support that suppression of HER2/AKT signaling plays an important role in itraconazole-mediated antitumor activity in esophageal cancer.

Itraconazole inhibits AKT activity in primary esophageal tumors in patients

We initiated a window-of-opportunity early phase I study to evaluate the feasibility of using itraconazole to treat resectable esophageal cancer patients in the neoadjuvant setting before CROSS trial based chemoradiation and surgery (37). Patients were given itraconazole 300 mg twice daily for 2 weeks prior to the initiation of standard-of-care chemoradiation (Supplementary Fig. S1). We chose two weeks because this was the typical time between diagnosis and either completion of a staging PET/CT scan or staging EUS and completion of radiation planning/simulation. Patients underwent endoscopic research biopsies of their tumor before and after itraconazole treatment, with one or both of the endoscopic procedures

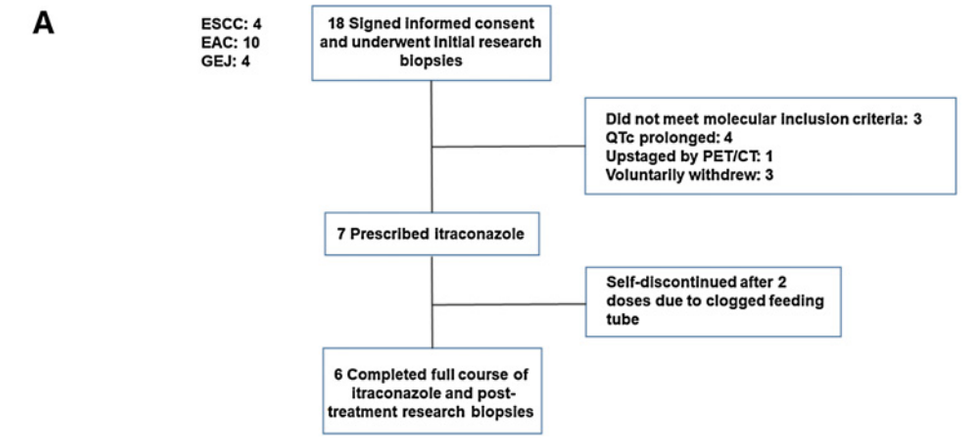

Patient	Tumor location	Histology	Clinical stage	Esophagectomy/findings	HER2 status	AE/SAE
A	Distal esophagus	AC	T3N1	Partial response, ypT3N2	3+, amplified	None
B	Distal esophagus	AC	T3N1	Pathologic CR, ypT0N0	1+, negative	None
C	Distal esophagus	AC	T3N2	Pathologic CR, yp T0N0	negative	None
D	Distal esophagus	AC	T3N0	Partial response, ypT3N0	3+, amplified	None
E	Distal esophagus	AC	T3N1	(Unresectable, positive radiographic response)	1+, negative	None
F	GE junction	AC	T3N0	(Refused surgery, positive radiographic response)	0, negative	None

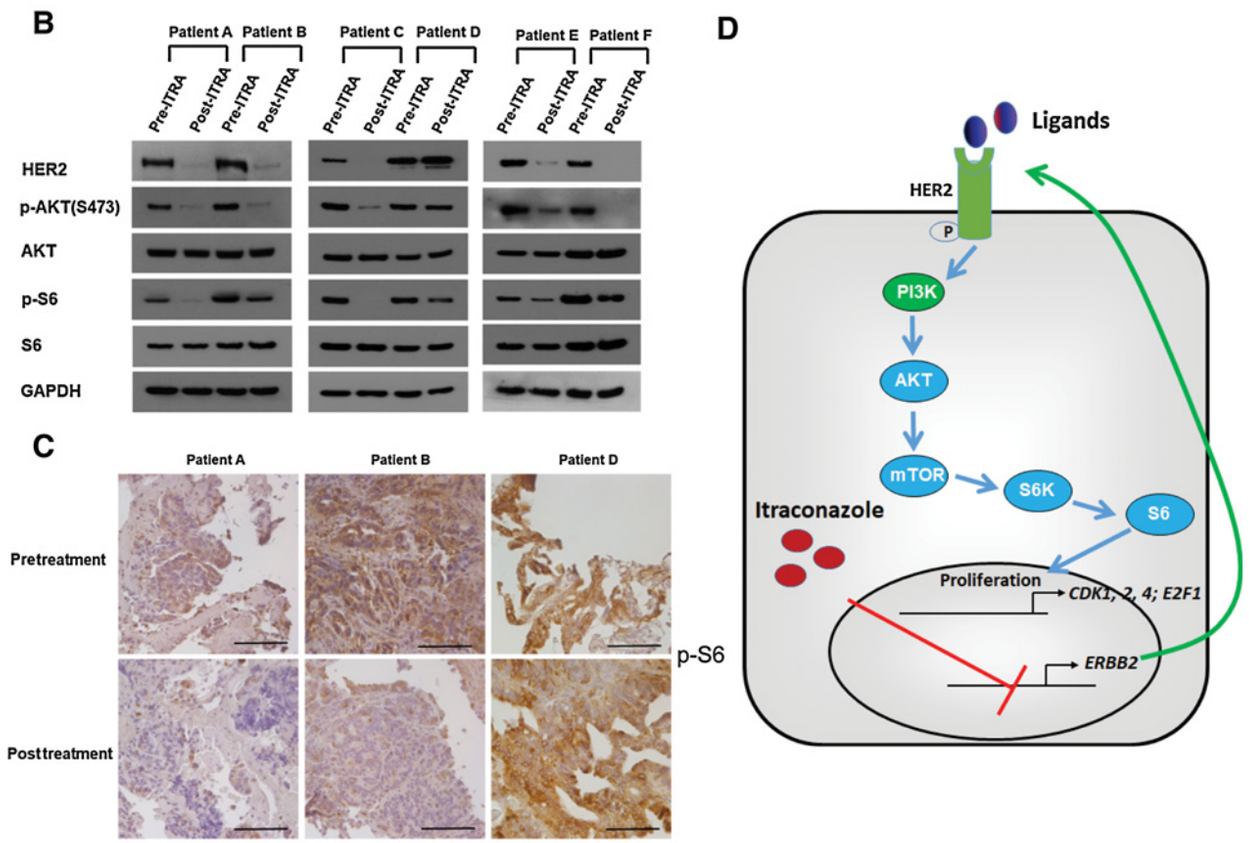

Figure 6.

Itraconazole inhibits HER2/AKT signaling in primary tumors from patients with esophageal cancer. **A,** Top, CONSORT diagram of early phase I trial. Eighteen patients with ESCC, EAC, or gastroesophageal junction cancer signed written informed consent and were enrolled in the trial. Following initial research biopsies but before itraconazole was prescribed, 11 patients screen failed or voluntarily withdrew. (*Continued on the following page.*)

considered standard of clinical care. Of 18 patients who provided written informed consent and enrolled in the trial, 11 patients failed screening for the treatment phase and one did not complete the full course of treatment. Tumors from the remaining six patients, white males between the ages of 61 and 72 with adenocarcinoma of the distal esophagus or gastroesophageal junction, who received the full course of itraconazole were analyzed (**Fig. 6A**). None of the six patients experienced either a related serious adverse event or a related adverse event during their itraconazole treatment course. We assessed the HER2-AKT signaling axis in paired pre- and post-itraconazole treated tumor biopsies by Western blot. Notably, we observed a marked decrease in the phosphorylation of AKT and its downstream effector S6 protein in five of six patients following itraconazole treatment (**Fig. 6B**). In addition, total HER2 protein was also decreased post itraconazole treatment in the five patients with decreased AKT and S6 protein phosphorylation. To demonstrate that decreased signaling occurred in tumor cells, biopsies were analyzed by immunohistochemistry for phosphorylated S6 protein expression. In patients A and B, the phosphorylated S6 protein staining was decreased after a 14-day course of itraconazole treatment (**Fig. 6C**). These positive results show that a short course of orally administered itraconazole inhibits HER2–AKT signaling in esophageal cancer tissue in human patients.

Discussion

In this report, we found that itraconazole effectively inhibited the proliferation of both ESCC and EAC cells by arresting them at the G_1–S transition of the cell cycle. This effect was mediated through downregulating *ERBB2* mRNA and downstream PI3K, AKT, and S6 phosphorylation and activation (**Fig. 6D**). To our knowledge, this is the first time the anti-tumor activity of itraconazole against human EAC has been shown. In mouse xenografts of EAC, itraconazole significantly decreased tumor growth along with total HER2 and phosphorylated AKT expression levels. Finally, we report the results of a pilot clinical trial (NCT02749513) testing the feasibility of administering oral itraconazole to patients with resectable EAC and the molecular effects on their primary esophageal tumors. Analysis of esophageal cancer specimens from patients with EAC treated with itraconazole confirmed itraconazole's efficacy in targeting HER2/AKT signaling within intact esophageal tumors. HER2 is amplified in roughly 30% of EAC, and in these patients trastuzumab can be beneficial (38). However, HER2 as a member of the EGFR family of RTK can be expressed in normal esophageal epithelium, ESCC, and EAC. In a Japanese study of 142 ESCC cases, 52.8% of the tumors expressed HER2 as determined by IHC (39). We found that pharmacologic inhibition of HER2 activity by lapatinib or siRNA-mediated knockdown of HER2 significantly reduced cell proliferation in ESCC and EAC cells.

Esophageal cancer is diagnosed in nearly half a million people worldwide each year and is the eighth leading cause of cancer-related death globally (5, 40, 41). Despite recent improvements in surgical technique, chemotherapy regimens, and radiation therapy, long-term survival of esophageal cancer remains poor (2). Thus, the development of novel molecularly targeted therapies could substantially improve survival. Currently only two molecularly targeted agents, trastuzumab (anti-HER2 antibody) and ramucirumab (anti-VEGFR2 antibody), are routinely used clinically in patients with advanced esophageal cancer (6, 7). Itraconazole, a commonly used antifungal agent, is a promising candidate as a molecularly targeted therapy in esophageal cancer. It was shown to reverse P-glycoprotein–mediated drug resistance associated with chemotherapy agents in the 1990s (11, 12). Itraconazole was later identified as a potent inhibitor of angiogenesis and Hedgehog signaling, both of which likely play a role in esophageal carcinogenesis, through screening a panel of more than 3,000 FDA-approved drugs (13, 14). Since then, a number of new clinical trials have been initiated to study its antitumor activity in a variety of solid tumors including basal cell carcinoma, non-small cell lung cancer, prostate cancer, and ovarian cancer (17–20, 22). A theoretical concern is that neoadjuvant itraconazole administration could induce antifungal resistance in patients who later develop systemic fungal infections in the peri-operative period. In general, postoperative invasive fungal infections are uncommon, with one study finding an incidence of 1.7% in ICU patients (42). While itraconazole resistance can occur in *Candida* and *Aspergillus*, this required nine months of therapy, a much longer treatment duration than used in our early phase I trial (43). Finally, in cases of fungal resistance to a specific azole antifungal drug, cross resistance does not necessarily occur with newer generation azole drugs or other classes of antifungals. While previous phase II studies administered itraconazole for longer times than we did (e.g., 2.3 months and 23.6 weeks), the number and severity of adverse events observed increased as treatment duration increased (17, 18). In addition, itraconazole interacts with many common drugs, in particular those metabolized by cytochrome P450 3A4. Thus, long-term use of itraconazole as an antineoplastic should be conducted under the direction of a knowledgeable healthcare provider and preferably in a clinical trial setting.

Serine/threonine kinase AKT is located at the crossroads of cell death and survival. It plays an essential role in multiple interconnected cell signaling pathways involved in cell proliferation and division, metabolism, epithelial–mesenchymal transition (EMT), genome stability, gene transcription, and protein synthesis. Studies have demonstrated that AKT signaling dysfunction occurs in various types of cancer and, in some cases, is associated with tumor metastases (33, 34). In recent years, aberrant signaling of this pathway and its involvement in the initiation and progression of esophageal cancer has been explored. Whole exome sequencing of esophageal cancer specimens has identified *AKT* gene amplification in approximately 20% of patients with ESCC (44, 45). Another study found activated *AKT* was increased in highly invasive esophageal cancer cell lines and that AKT signaling contributed to ESCC metastases (46). A clinical study found *AKT* mRNA was markedly overexpressed in tumor tissue compared with adjacent normal cells (47). Here, our results showed that phospho-AKT expression was increased in both ESCC and EAC cell lines

(*Continued.*) Seven patients were prescribed itraconazole, with one patient discontinuing the medication after only 2 doses. Bottom: clinical and pathologic characteristics of the 6 patients who completed the full course of itraconazole. **B,** Western blot analysis of p-AKT, AKT, p-S6, S6, and HER2 protein in primary tumors from 6 patients with esophageal cancer before and after itraconazole treatment. GAPDH is used as a loading control. **C,** IHC staining of p-S6 from representative tumor sections of three different patients before (top) and after (bottom) itraconazole treatment. Patients A and B responded while patient D minimally responded. Scale bar, 100 μm. **D,** Schematic diagram of itraconazole's action in esophageal cancer. HER2 functional activation promotes PI3K/AKT/mTOR/S6 signaling, leading to the upregulation of AKT signaling target genes *CDK1, CDK2, CDK4*, and *E2F1*. Itraconazole suppresses this signaling pathway through downregulating *ERBB2* mRNA.

compared with benign esophageal cell lines. We found that pharmacological inhibition of AKT activity significantly reduced cell proliferation in esophageal cancer cells. AKT target genes *CDK1, CDK2, CDK4*, and *E2F1* were significantly decreased following itraconazole treatment. A recent study in ESCC showed that itraconazole treatment led to the inhibition of cancer cell growth through activation of AMPK (24). Surprisingly, we did not observe increased phosphorylation of AMPK either in four cell lines or in xenografts following itraconazole treatment. This may be due to innate differences found in ESCC cell lines. In our study, we clearly demonstrated that the reduced phosphorylation of AKT was due to decreased activity of its upstream kinase PI3K. Moreover, we provided evidence that itraconazole decreased expression of HER2/ERBB2 at both the messenger RNA and protein level, which resulted in decreased activity of PI3K. However, we cannot exclude the possibility that itraconazole also targets other RTKs to downregulate PI3K and AKT activity. Future studies should investigate the molecular mechanism by which itraconazole represses *ERBB2* expression at the transcriptional level. Together, our data along with others suggest that HER2/AKT is a promising and viable therapeutic target in esophageal cancer.

Esophageal cancer is known to be a highly angiogenic tumor. VEGFR2 binds VEGF to mediate tumor angiogenesis. The human IgG1 recombinant mAb ramucirumab that targets VEGFR2 is FDA-approved for use in metastatic gastric or gastroesophageal junction cancer, and clinical guidelines include its use in EAC. Zhang and colleagues previously demonstrated the existence of a VEGF autocrine signaling loop, in which VEGF binds to VEGFR2 activating signaling in esophageal cancer cell lines (48). Our finding that itraconazole inhibits esophageal cancer cell growth via an AKT-dependent mechanism does not exclude the possibility that itraconazole also suppresses other signaling pathways including VEGFR2. In cancer therapy, there is a general agreement that molecules interfering simultaneously with multiple signaling pathways might be more effective than agents that have a single molecular target. Thus, itraconazole has great potential to be repurposed as a molecularly targeted therapy for esophageal cancer. A better understanding of whether and how receptor tyrosine kinases and angiogenic signaling contribute to itraconazole-dependent antitumor activity in esophageal cancer is an important area for future study.

Finally, based on the results of our pilot study demonstrating that orally administered itraconazole inhibits HER2/AKT signaling in intact esophageal tumors with an absence of adverse events in our patients, we have launched a phase II trial (NCT04018872) to evaluate the therapeutic effect of itraconazole on esophageal tumors. Following the completion of neoadjuvant chemoradiation, patients with resectable esophageal cancer will be given itraconazole 300 mg twice daily for 6–8 weeks before undergoing esophagectomy. At the time of esophagectomy, esophageal tissue will be harvested to determine itraconazole and hydroxyitraconazole levels. We hypothesize that itraconazole will improve pathologic complete response rates in esophageal cancer based on the results from our early phase I trial.

Authors' Disclosures

K.B. Dunbar reports grants from Department of Veterans Affairs VA MERIT CSR&D during the conduct of the study; grants from Ironwood Pharmaceuticals outside the submitted work. M.S. Beg reports personal fees from Ipsen, Merck, AZ, FMI, outside the submitted work. J. Kim reports grants from NCI and grants from American Cancer Society during the conduct of the study; personal fees from COTA Inc outside the submitted work. J.E. Dowell reports personal fees from Astra Zeneca during the conduct of the study; personal fees from Physicians Education Resource outside the submitted work. W.C. Putnam reports grants from Cancer Prevention & Research Institute of Texas during the conduct of the study. D.H. Wang reports grants from US NIDDK and grants from Friends of the Simmons Comprehensive Cancer Center during the conduct of the study. No disclosures were reported by the other authors.

Authors' Contributions

W. Zhang: Conceptualization, data curation, formal analysis, validation, investigation, writing–original draft, writing–review and editing. **A.S. Bhagwath:** Data curation, investigation. **Z. Ramzan:** Data curation, formal analysis, investigation. **T.A. Williams:** Data curation, investigation. **I. Subramaniyan:** Data curation, investigation. **V. Edpuganti:** Data curation, investigation. **R.R. Kallem:** Data curation, investigation. **K.B. Dunbar:** Resources, data curation, funding acquisition, investigation. **P. Ding:** Data curation, investigation. **K. Gong:** Data curation, Investigation. **S.A. Geurkink:** Data curation. **M.S. Beg:** Conceptualization. **J. Kim:** Conceptualization, investigation. **Q. Zhang:** Data curation, investigation. **A.A. Habib:** Resources, funding acquisition. **S.-H. Choi:** Data curation, investigation. **R. Lapsiwala:** Data curation, investigation. **G. Bhagwath:** Data curation, investigation. **J.E. Dowell:** Resources, data curation, investigation. **S.D. Melton:** Data curation, validation, investigation. **C. Jie:** Formal analysis, methodology. **W.C. Putnam:** Resources, data curation, formal analysis, supervision, funding acquisition, investigation. **T.H. Pham:** Conceptualization, formal analysis, investigation. **D.H. Wang:** Conceptualization, resources, data curation, formal analysis, supervision, funding acquisition, validation, investigation, visualization, methodology, writing–original draft, project administration, writing–review and editing.

Acknowledgments

We thank Sanjai Sabu, Jessica Vallejo, Pooja Dalal, and Mary Mason for regulatory, clinical coordination, and patient data management assistance. This work was supported by a New Investigator Award (to W. Zhang) from the VA North Texas Health Care System, the U.S. Department of Veterans Affairs 5I01CX001668 (to K.B. Dunbar) and 2I01BX002559–07 (to A.A. Habib); the NIH 1R01CA196851 (to J. Kim), 1R01CA244212–01A1 (to A.A. Habib) and R01-DK97340 (to D.H. Wang), the Cancer Prevention Research Institute of Texas Core Facilities Support Award RP170003 (to W.C. Putnam), the American Cancer Society ACS-RSG-16–090–01-TBG (to J. Kim), and the Friends of the Simmons Comprehensive Cancer Center (to D.H. Wang).

The costs of publication of this article were defrayed in part by the payment of page charges. This article must therefore be hereby marked *advertisement* in accordance with 18 U.S.C. Section 1734 solely to indicate this fact.

Received July 28, 2020; revised February 11, 2021; accepted July 30, 2021; published first August 10, 2021.

References

1. Bray F, Ferlay J, Soerjomataram I, Siegel RL, Torre LA, Jemal A. Global cancer statistics 2018: GLOBOCAN estimates of incidence and mortality worldwide for 36 cancers in 185 countries. CA Cancer J Clin 2018;68:394–424.
2. Dubecz A, Gall I, Solymosi N, Schweigert M, Peters JH, Feith M, et al. Temporal trends in long-term survival and cure rates in esophageal cancer: a SEER database analysis. J Thorac Oncol 2012;7:443–7.
3. Rustgi AK, El-Serag HB. Esophageal carcinoma. N Engl J Med 2014;371: 2499–509.
4. Zhang W, Wang DH. Origins of Metaplasia in Barrett's Esophagus: Is this an Esophageal Stem or Progenitor Cell Disease? Dig Dis Sci 2018;63:2005–12.
5. Ajani JA, D'Amico TA, Bentrem DJ, Chao J, Corvera C, Das P, et al. Esophageal and esophagogastric junction cancers, version 2.2019, NCCN clinical practice guidelines in oncology. J Natl Compr Canc Netw 2019;17:855–83.
6. Bang YJ, Van Cutsem E, Feyereislova A, Chung HC, Shen L, Sawaki A, et al. Trastuzumab in combination with chemotherapy versus chemotherapy alone for treatment of HER2-positive advanced gastric or gastro-oesophageal junction cancer (ToGA): a phase 3, open-label, randomised controlled trial. Lancet 2010; 376:687–97-X.
7. Fuchs CS, Tomasek J, Yong CJ, Dumitru F, Passalacqua R, Goswami C, et al. Ramucirumab monotherapy for previously treated advanced gastric or gastro-

oesophageal junction adenocarcinoma (REGARD): an international, randomised, multicentre, placebo-controlled, phase 3 trial. Lancet 2014;383:31–9.
8. Moehler MH, Janjigian YY, Adenis A, Aucoin J-S, Boku N, Chau I, et al. CheckMate 649: A randomized, multicenter, open-label, phase III study of nivolumab (NIVO) + ipilimumab (IPI) or nivo + chemotherapy (CTX) versus CTX alone in patients with previously untreated advanced (Adv) gastric (G) or gastroesophageal junction (GEJ) cancer. J Clin Oncol 2018;36(4_suppl): TPS192–TPS.
9. Kato K, Cho BC, Takahashi M, Okada M, Lin CY, Chin K, et al. Nivolumab versus chemotherapy in patients with advanced oesophageal squamous cell carcinoma refractory or intolerant to previous chemotherapy (ATTRACTION-3): a multicentre, randomised, open-label, phase 3 trial. Lancet Oncol 2019;20:1506–17.
10. Kato K, Shah MA, Enzinger P, Bennouna J, Shen L, Adenis A, et al. KEYNOTE-590: Phase III study of first-line chemotherapy with or without pembrolizumab for advanced esophageal cancer. Future Oncol 2019;15: 1057–66.
11. Kurosawa M, Okabe M, Hara N, Kawamura K, Suzuki S, Sakurada K, et al. Reversal effect of itraconazole on adriamycin and etoposide resistance in human leukemia cells. Ann Hematol 1996;72:17–21.
12. Takara K, Tanigawara Y, Komada F, Nishiguchi K, Sakaeda T, Okumura K. Cellular pharmacokinetic aspects of reversal effect of itraconazole on P-glycoprotein-mediated resistance of anticancer drugs. Biol Pharm Bull 1999;22:1355–9.
13. Chong CR, Xu J, Lu J, Bhat S, Sullivan DJ Jr., Liu JO. Inhibition of angiogenesis by the antifungal drug itraconazole. ACS Chem Biol 2007;2:263–70.
14. Kim J, Tang JY, Gong R, Kim J, Lee JJ, Clemons KV, et al. Itraconazole, a commonly used antifungal that inhibits Hedgehog pathway activity and cancer growth. Cancer Cell 2010;17:388–99.
15. Pantziarka P, Sukhatme V, Bouche G, Meheus L, Sukhatme VP. Repurposing Drugs in Oncology (ReDO)-itraconazole as an anti-cancer agent. Ecancermedicalscience 2015;9:521.
16. Pounds R, Leonard S, Dawson C, Kehoe S. Repurposing itraconazole for the treatment of cancer. Oncol Lett 2017;14:2587–97.
17. Kim DJ, Kim J, Spaunhurst K, Montoya J, Khodosh R, Chandra K, et al. Open-label, exploratory phase II trial of oral itraconazole for the treatment of basal cell carcinoma. J Clin Oncol 2014;32:745–51.
18. Antonarakis ES, Heath EI, Smith DC, Rathkopf D, Blackford AL, Danila DC, et al. Repurposing itraconazole as a treatment for advanced prostate cancer: a noncomparative randomized phase II trial in men with metastatic castration-resistant prostate cancer. Oncologist 2013;18:163–73.
19. Rudin CM, Brahmer JR, Juergens RA, Hann CL, Ettinger DS, Sebree R, et al. Phase 2 study of pemetrexed and itraconazole as second-line therapy for metastatic nonsquamous non-small-cell lung cancer. J Thorac Oncol 2013;8: 619–23.
20. Gerber DE, Putnam WC, Fattah FJ, Kernstine KH, Brekken RA, Pedrosa I, et al. Concentration-dependent early antivascular and antitumor effects of itraconazole in non-small cell lung cancer. Clin Cancer Res 2020;26:6017–27.
21. Tsubamoto H, Sonoda T, Inoue K. Impact of itraconazole on the survival of heavily pre-treated patients with triple-negative breast cancer. Anticancer Res 2014;34:3839–44.
22. Tsubamoto H, Sonoda T, Yamasaki M, Inoue K. Impact of combination chemotherapy with itraconazole on survival of patients with refractory ovarian cancer. Anticancer Res 2014;34:2481–7.
23. Tsubamoto H, Sonoda T, Ikuta S, Tani S, Inoue K, Yamanaka N. Combination chemotherapy with itraconazole for treating metastatic pancreatic cancer in the second-line or additional setting. Anticancer Res 2015;35:4191–6.
24. Chen MB, Liu YY, Xing ZY, Zhang ZQ, Jiang Q, Lu PH, et al. Itraconazole-induced inhibition on human esophageal cancer cell growth requires AMPK activation. Mol Cancer Ther 2018;17:1229–39.
25. Kelly RJ, Ansari AM, Miyashita T, Zahurak M, Lay F, Ahmed AK, et al. Targeting the Hedgehog Pathway Using Itraconazole to Prevent Progression of Barrett's Esophagus to Invasive Esophageal Adenocarcinoma. Ann Surg 2021;273:e206–13.
26. Zhang Q, Agoston AT, Pham TH, Zhang W, Zhang X, Huo X, et al. Acidic bile salts induce epithelial to mesenchymal transition via VEGF signaling in non-neoplastic Barrett's cells. Gastroenterology 2019;156:130–44.
27. Zhang W, Hong S, Maniar KP, Cheng S, Jie C, Rademaker AW, et al. KLF13 regulates the differentiation-dependent human papillomavirus life cycle in keratinocytes through STAT5 and IL-8. Oncogene 2016;35:5565–75.
28. Zhang W, Williams TA, Bhagwath AS, Hiermann JS, Peacock CD, Watkins DN, et al. GEAMP, a novel gastroesophageal junction carcinoma cell line derived from a malignant pleural effusion. Lab Invest 2020;100:16–26.
29. Zhang W, Zeng X, Briggs KJ, Beaty R, Simons B, Chiu Yen RW, et al. A potential tumor suppressor role for Hic1 in breast cancer through transcriptional repression of ephrin-A1. Oncogene 2010;29:2467–76.
30. Pham TH, Melton SD, McLaren PJ, Mokdad AA, Huerta S, Wang DH, et al. Laparoscopic ischemic conditioning of the stomach increases neovascularization of the gastric conduit in patients undergoing esophagectomy for cancer. J Surg Oncol 2017;116:391–7.
31. Hu Q, Hou YC, Huang J, Fang JY, Xiong H. Itraconazole induces apoptosis and cell cycle arrest via inhibiting Hedgehog signaling in gastric cancer cells. J Exp Clin Cancer Res 2017;36:50.
32. Wang X, Wei S, Zhao Y, Shi C, Liu P, Zhang C, et al. Anti-proliferation of breast cancer cells with itraconazole: Hedgehog pathway inhibition induces apoptosis and autophagic cell death. Cancer Lett 2017;385:128–36.
33. Vivanco I, Sawyers CL. The phosphatidylinositol 3-Kinase AKT pathway in human cancer. Nat Rev Cancer 2002;2:489–501.
34. Hoxhaj G, Manning BD. The PI3K-AKT network at the interface of oncogenic signalling and cancer metabolism. Nat Rev Cancer 2020;20:74–88.
35. Sarbassov DD, Guertin DA, Ali SM, Sabatini DM. Phosphorylation and regulation of Akt/PKB by the rictor-mTOR complex. Science 2005;307:1098–101.
36. Hardie DG. Minireview: the AMP-activated protein kinase cascade: the key sensor of cellular energy status. Endocrinology 2003;144:5179–83.
37. Shapiro J, van Lanschot JJB, Hulshof M, van Hagen P, van Berge Henegouwen MI, Wijnhoven BPL, et al. Neoadjuvant chemoradiotherapy plus surgery versus surgery alone for oesophageal or junctional cancer (CROSS): long-term results of a randomised controlled trial. Lancet Oncol 2015;16:1090–8.
38. Iqbal N, Iqbal N. Human epidermal growth factor receptor 2 (HER2) in cancers: overexpression and therapeutic implications. Mol Biol Int 2014;2014:852748.
39. Yamamoto Y, Yamai H, Seike J, Yoshida T, Takechi H, Furukita Y, et al. Prognosis of esophageal squamous cell carcinoma in patients positive for human epidermal growth factor receptor family can be improved by initial chemotherapy with docetaxel, fluorouracil, and cisplatin. Ann Surg Oncol 2012;19:757–65.
40. Ajani JA, Barthel JS, Bentrem DJ, D'Amico TA, Das P, Denlinger CS, et al. Esophageal and esophagogastric junction cancers. J Natl Compr Canc Netw 2011;9:830–87.
41. Ajani JA, D'Amico TA, Almhanna K, Bentrem DJ, Besh S, Chao J, et al. Esophageal and esophagogastric junction cancers, version 1.2015. J Natl Compr Canc Netw 2015;13:194–227.
42. Pittet D, Monod M, Suter PM, Frenk E, Auckenthaler R. Candida colonization and subsequent infections in critically ill surgical patients. Ann Surg 1994;220: 751–8.
43. Denning DW, Venkateswarlu K, Oakley KL, Anderson MJ, Manning NJ, Stevens DA, et al. Itraconazole resistance in Aspergillus fumigatus. Antimicrob Agents Chemother 1997;41:1364–8.
44. Cancer Genome Atlas Research Network, Analysis Working Group: Asan University, BC Cancer Agency, Brigham and Women's Hospital, Broad Institute, et al. Integrated genomic characterization of oesophageal carcinoma. Nature 2017;541:169–75.
45. Chen XX, Zhong Q, Liu Y, Yan SM, Chen ZH, Jin SZ, et al. Genomic comparison of esophageal squamous cell carcinoma and its precursor lesions by multi-region whole-exome sequencing. Nat Commun 2017;8:524.
46. Li B, Xu WW, Lam AKY, Wang Y, Hu HF, Guan XY, et al. Significance of PI3K/AKT signaling pathway in metastasis of esophageal squamous cell carcinoma and its potential as a target for anti-metastasis therapy. Oncotarget 2017;8: 38755–66.
47. Saeed N, Shridhar R, Hoffe S, Almhanna K, Meredith KL. AKT expression is associated with degree of pathologic response in adenocarcinoma of the esophagus treated with neoadjuvant therapy. J Gastrointest Oncol 2016;7:158–65.
48. Zhang Q, Yu C, Peng S, Xu H, Wright E, Zhang X, et al. Autocrine VEGF signaling promotes proliferation of neoplastic Barrett's epithelial cells through a PLC-dependent pathway. Gastroenterology 2014;146:461–72.